BIOCHEMICAL PHARMACOLOGY 77 (2009) 337–347

available at www.sciencedirect.com

ScienceDirect

journal homepage: www.elsevier.com/locate/biochempharm

trans-Resveratrol inhibits H_2O_2-induced adenocarcinoma gastric cells proliferation via inactivation of MEK1/2-ERK1/2-c-Jun signalling axis

Katia Aquilano [a], *Sara Baldelli* [a], *Giuseppe Rotilio* [a,b], *Maria Rosa Ciriolo* [a,b,*]

[a] *Department of Biology, University of Rome "Tor Vergata", Via della Ricerca Scientifica, 00133 Rome, Italy*
[b] *Research Center IRCCS San Raffaele, Via dei Bonacolsi, 00165 Rome, Italy*

ARTICLE INFO

Article history:
Received 2 September 2008
Accepted 14 October 2008

Keywords:
Hydrogen peroxide
ERK1/2
Resveratrol
c-Jun
Cell proliferation

ABSTRACT

In this report we investigate the signalling pathway activated by H_2O_2 in human adenocarcinoma gastric cells (AGS) and we evaluate the anti-proliferative action of the natural stilbene *trans*-resveratrol. We demonstrate that H_2O_2 accelerates cell growth and induces a prompt MEK1/2-ERK1/2 activation. Such events are also associated with the activation of c-Jun and its translocation into the nuclear compartment. A specific inhibitor of ERK1/2 phosphorylation by MEK1/2 (U0126) abrogates these phenomena. On the contrary, specific inhibition of JNK activity does not influence H_2O_2-mediated growth, suggesting that cell proliferation likely proceeds via MEK1/2-ERK1/2-Jun signalling axis. *trans*-Resveratrol is also able to completely suppress the increase in proliferation. We demonstrate that this property is not due to its antioxidant capacity but rather due to a specific inhibition of ERK1/2 phosphorylation by MEK1/2 and repression of c-Jun activation.

1. Introduction

Reactive oxygen species (ROS) have been historically considered toxic molecules able to induce an indiscriminate oxidative damage to biological macromolecules, and thus viewed as primary determinants of several pathological conditions and aging [1,2]. ROS are potential carcinogens because they can provoke DNA damages that lead to genomic instability and possibly stimulate cancer progression [3]. Nevertheless, it is now well established that ROS have been designed by evolution to participate in the maintenance of cellular homeostasis, functioning as second messengers in diverse signalling pathways [4]. Previous reports showed that at low concentration ROS (in particular H_2O_2 and $O_2^{\bullet-}$) can enhance the growth of many cellular types including tumour cells [5,6]. On the contrary, high concentration of ROS can cause oxidative stress and inhibit cell proliferation inducing apoptosis. Overall these processes are modulated by the activation of ROS-sensitive mitogen activated protein kinases (MAPKs) [7]. MAPKs is a family of proteins promoting a phosphorylative signalling cascade that culminates in the activation of transcription factors involved either in cellular proliferation or apoptosis [8].

Gastric cancer is one of the leading causes of cancer mortality worldwide. Chemotherapy is currently the preferential and more efficient treatment option although it often fails due to the development of multidrug resistance and recurrence of secondary tumours [9]. Given that many cancer cells display a significant alteration of intracellular redox balance, redox drugs have been designed to selectively kill transformed cells [10]. The use of diet-derived phytochemicals has been proposed as a valid strategy for both cancer prevention and treatment [11]. Actually, a wide variety of

* *Corresponding author at*: Department of Biology, University of Rome "Tor Vergata", Via della Ricerca Scientifica, 1, 00133 Rome, Italy. Tel.: +39 06 72594360; fax: +39 067259 4311.
E-mail address: ciriolo@bio.uniroma2.it (M.R. Ciriolo).
0006-2952/$ – see front matter
doi:10.1016/j.bcp.2008.10.034

studies suggest that regular consumption of fruits and vegetables is inversely associated with cancer risk [12]. The protective action of fruits and vegetables has been suggested to rely on their high content of antioxidant vitamins and polyphenols, which are released during the digestion in the gastro-intestinal tract [13]. Therefore, they could be of relevance for gastric cancer prevention/treatment. Among phytochemicals, polyphenols have been indicated to have significant chemotherapeutic potential by virtue of their pro-oxidant action. Stilbene *trans*-resveratrol (RV) is one of the most studied polyphenol present in the skin of red grapes and various other foods [14]. RV is a promising natural molecule for cancer prevention and treatment by virtue of its double action as pro- or antioxidant agent [15]. Indeed, similarly to other dietary polyphenols, RV has been reported to undergo oxidation and generate ROS [16], especially at high concentration and/or in the presence of transition metals and to be effective in arresting proliferation in a number of tumour cells via redox-dependent pathways [14,17]. RV can also function as antioxidant both in *in vivo* and *in vitro* [18–20], thus inhibiting tumour cells growth by counteracting ROS-driven proliferation. However, many polyphenols are able to strongly inhibit MAPKs via a mechanism that does not involve their redox activity. Quercetin and miricetin inhibit MEK-ERK signalling more effectively than well-known pharmacologic inhibitors of MEK1/2 [21,22], presumably by stabilizing the inactive conformation of the activation loop of the kinase [22]. Data reported on RV are still contradictory. For instance, RV seems to have no effect on MEK1 activity in transformed mouse epithelial cells [22], whereas it interferes with ERK1/2 phosphorylation and AP1 transcriptional activity in human smooth muscle epidermoid carcinoma cells [23,24].

In this study, we characterized the anti-proliferative effect of low doses of RV in adenocarcinoma gastric cells (AGS). We demonstrated that proliferation proceeds via the ERK1/2-c-Jun signalling cascade and that it is significantly abolished by RV through specific inhibition of MEK1/2-mediated ERK1/2 phosphorylation.

2. Materials and methods

2.1. Reagents

Hydrogen peroxide (H_2O_2), bovine catalase, proteases inhibitor cocktail, anti-β-tubulin, dithiothreitol (DTT), dimethylsulfoxide (DMSO), seleno-methionine, *trans*-resveratrol were from Sigma–Aldrich (St. Louis, MO, USA). Polyclonal anti-ERK1, anti-c-Jun antibodies, and monoclonal anti-p-c-Jun (Ser63), anti-p-JNK (Thr183, Tyr 185) antibodies were from Santa Cruz Biotecnology (Santa Cruz, CA, USA). JNK inhibitor I and MEK1/2 inhibitor (U0126) were from Calbiochem-Novabiochem Corporation (La Jolla, CA, USA). Polyclonal anti-p-ERK1/2 and p-MEK1/2 antibodies were from Cell Signalling (Beverly, MA, USA). MTS assay kit ''CellTiter 96 AQ_{ueous} One Solution Cell Proliferation Assay'' was purchased from Promega (Madison, WI). IgG (H + L)-HRP-conjugate anti-mouse and anti-rabbit secondary antibodies, and nitrocellulose membranes were from Bio-Rad Laboratories (Hercules, CA, USA). ChemiGlow chemiluminescence substrate was from Alpha Innotech Corporation (San Leandro, CA, USA). BrdU Cell Proliferation assay kit was from GE Healthcare (Buckinghamshire, UK). All other chemicals were obtained from Merck (Darmstadt, Germany).

2.2. Cell cultures

Human adenocarcinoma gastric cells were purchased from the European Collection of Cell Cultures (Salisbury, UK). AGS cells were grown in F12 medium supplemented with 10% FCS (Lonza, Basel, CH), 2 mM glutamine, 100 U/ml penicillin/streptomycin and maintained at 37 °C in an atmosphere of 5% CO_2 in air.

2.3. Analysis of cell viability and proliferation

Adherent (after trypsinization) and detached cells were combined, washed with PBS and directly counted by optical microscope on hemocytometer after Trypan Blue staining. Alternatively, cell proliferation was measured by using a MTS assay kit ''Cell Titer 96® Aqueous One Solution Cell Proliferation assay'' (Promega) according to the manufacturer's instructions. Cell proliferation was also assayed by a ''Cell Proliferation kit'' (Buckinghamshire, UK) based on the immunocytochemical detection of 5-bromo-2′-deoxyuridine (BrdU) incorporated into cellular DNA of proliferating cells. Cells were stained as previously described [25].

2.4. Treatments

Treatments with H_2O_2 were performed with different concentrations ranging from 10 to 50 μM at 37 °C in culture medium. The concentration of 20 μM H_2O_2 was selected for all of the experiments as it gave the most significant degree of proliferation. Treatments at concentrations higher than 50 μM resulted cytotoxic. Treatment with the cell-permeable MEK1/2 inhibitor U0126 or JNK inhibitor I was done at the concentration of 260 nM and 10 μM respectively. These inhibitors were added 1 h before H_2O_2 treatment and maintained throughout the experiment. RV (dissolved in DMSO) was used at the concentration of 500 nM because higher concentrations were cytotoxic. RV was added 1 h prior H_2O_2 treatment and maintained throughout the experiment. As control, equal amount of DMSO (0.1%) was added to untreated cells. Catalase was added 1 h prior H_2O_2 treatment at the concentration of 1 μM and maintained throughout the experiment.

Treatment with 0.1 μg/ml seleno-methionine was carried out to induce the expression and activity levels of glutathione peroxidase (GPx) as previously described [26]. Prior H_2O_2 treatment the medium containing seleno-methionine was removed and replaced with fresh medium.

2.5. Western blot analyses

1×10^6 cells were washed twice with cold PBS and harvested by centrifugation at $1000 \times g$ for 5 min at 4 °C. Nuclear protein fraction were obtained as previously described [25]. Alternatively, total protein extracts were obtained by lysing 1×10^5 cells in 100 μl Laemmli buffer. Total (30 μl), supernatant (20 μg), or nuclear proteins (20 μg) were electrophoresed on 8.5%

or 10% SDS-polyacrylamide gels and blotted onto nitrocellulose. Membranes were stained with primary antibodies against, p-ERK1/2 (1:500), p-MEK1/2 (1:1000), ERK1/2 (1:500), c-Jun (1:1000), p-c-Jun (1:500), JNK (1:1000), p-JNK (1:500) or β-tubulin (1:5000). After incubation with the appropriate HRP-conjugate secondary antibodies (Bio-Rad Laboratories, Hercules, CA, USA), protein bands were detected using a Fluorchem Imaging system (Alpha Innotech Corporation-Analitica De Mori, Italy) upon staining with ChemiGlow chemiluminescence substrate. Densitometric analyses of protein bands were performed by the Quantity one software (Bio-Rad). β-Tubulin was used as loading control. Proteins were assayed by the method of Lowry [27].

2.6. Determination of ROS

ROS were detected by cytofluorimetric analysis after incubation for 1 h at 37 °C with 50 μM DCF-DA. After treatment, cells were scraped, washed and resuspended in PBS. The fluorescence intensities of 10,000 cells from each sample were detected by FACScalibur instrument (Beckton and Dickinson, San Josè, CA). Data were analyzed using the WinMDI 2.8 software.

2.7. Statistical analysis

The results are presented as means ± S.D. Statistical evaluation was conducted by ANOVA, followed by the post hoc Student–Newman–Keuls. Differences were considered to be significant at $p < 0.05$.

3. Results

3.1. Low doses of H_2O_2 induced AGS cell proliferation

In the last years, many studies have reported that application of physiologic levels of H_2O_2 to mammalian cells stimulate biological responses and activate specific biochemical pathways. In particular, H_2O_2 has been demonstrated to increase the proliferation of normal and cancer cells by different signalling pathways [6]. In the present work, we investigated the effect of H_2O_2 on the proliferation rate of human AGS cells. Cells were treated with different concentration of H_2O_2 and MTS assay was carried out after 24 h. As showed in Fig. 1A, H_2O_2 at the concentration of 10 μM was already able to significantly increase cell proliferation (+40%), with a more

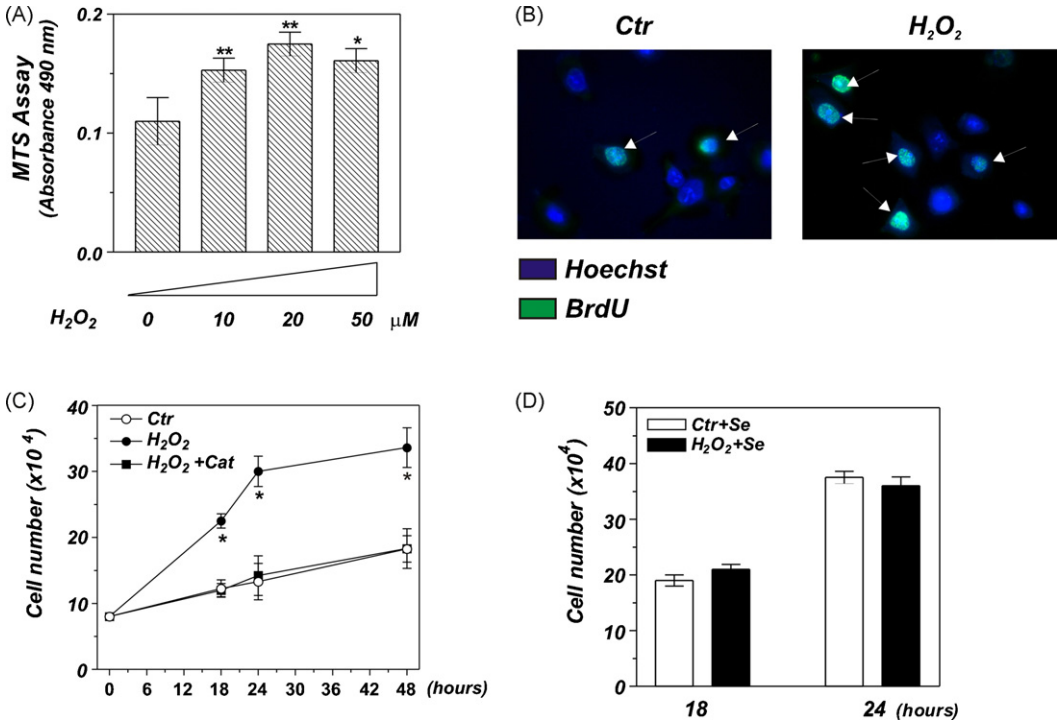

Fig. 1 – H_2O_2 accelerates AGS cells proliferation. (A) Cells proliferation was assayed by MTS, 24 h after treatment with the indicated concentrations of H_2O_2. Data are expressed as means ± S.D. ($n = 10$; $^*p < 0.01$; $^{**}p < 0.001$). (B) Cell proliferation was determined by immunofluorescence detection of incorporated BrdU (green), as described under Section 2, 6 h after treatment with 20 μM H_2O_2. Nuclei were stained with Hoechst 33342 (blue). Images reported are from one experiment representative of three that gave similar results. White arrows indicate the BrdU-positive cells. (C) Cells number was determined by Trypan Blue exclusion after 20 μM H_2O_2 treatment. 1 μM catalase (Cat) was added in culture medium 1 h prior H_2O_2 and maintained throughout the experiment. Data are expressed as means ± S.D. ($n = 6$; $^*p < 0.001$ *versus* control cells). (D) AGS cells were cultured in the presence of 0.1 μM seleno-methionine (Se) for 3 weeks. Medium containing seleno-methionine was removed just before the experiment and replaced with fresh medium. Cell growth was determined by Trypan Blue exclusion after treatment with 20 μM H_2O_2 for 24 h. Data are expressed as means ± S.D. ($n = 4$). (For interpretation of the references to color in this figure legend, the reader is referred to the web version of the article.)

pronounced effect at 20 μM (+60%), whereas a decrease in the growth rate was observed at 50 μM (+46%). Therefore, we selected the concentration of 20 μM H_2O_2 for all the experiments. Anti-BrdU immunohistochemistry was then employed to confirm the data obtained by MTS test. Fig. 1B shows that 6 h after H_2O_2 addition, approximately 55% of cells incorporated BrdU (cells in S phase), whereas only about 14% of control cells stained positively. The effects of H_2O_2 on AGS cells proliferation were further analyzed by direct counts upon Trypan Blue exclusion. Cell number determined up to 48 h was increased upon treatment with 20 μM H_2O_2 particularly between 18 and 24 h (Fig. 1C) without any changes in the number of Trypan Blue positive cells (data not shown). Treatment with catalase, an enzyme that efficiently scavenges H_2O_2, completely abrogated the increase in proliferation, confirming the H_2O_2-mediated effect (Fig. 1C). We then verified whether by increasing the intracellular H_2O_2-scavenging capacity the proliferative effect could be also inhibited. Therefore, H_2O_2 treatment was carried out on AGS cells previously grown for 3 weeks in culture medium supplemented with 0.1 μg/ml seleno-methionine, a condition that we previously demonstrated to increase the expression and the activity levels of glutathione peroxidase [26]. Fig. 1D shows that, under these conditions, AGS cells were insensitive to H_2O_2 treatment as no difference in the growth rate was detected with respect to untreated cells.

3.2. H_2O_2 induced ERK1/2 phosphorylation in AGS cells

To delineate the signalling pathway(s) through which H_2O_2 evoked AGS cells growth, we assessed the ability of H_2O_2 to activate MAPKs. We considered ERK1/2, a pro-survival H_2O_2-sensitive MAPK majorly stimulating cell proliferation. In particular, we determined the effect of 20 μM H_2O_2 on the

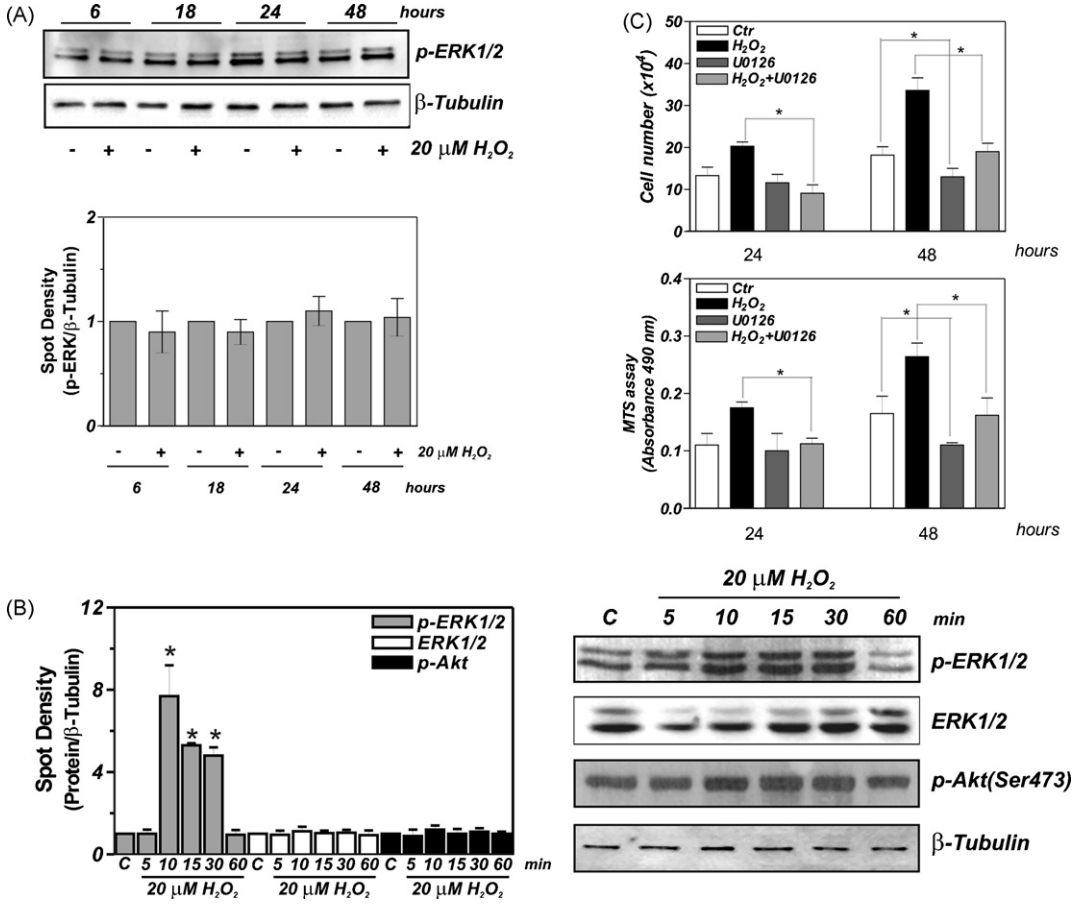

Fig. 2 – H_2O_2-evoked cell proliferation was associated with activation of ERK1/2. (A) AGS cells were treated with 20 μM H_2O_2 for the indicated times. p-ERK1/2 was detected by Western blot on total protein extracts. Immunoblots reported are from one experiment representative of four that gave similar results. β-Tubulin was used as loading control. Density of immunoreactive bands was calculated using the software Quantity one (Bio-Rad) and data are shown as ratio of p-ERK/β-tubulin. Data are expressed as means ± S.D. ($n = 4$). (B) AGS cells were treated with 20 μM H_2O_2 for the indicated times. p-ERK1/2, ERK1/2 and p-Akt were detected by Western blot on total protein extracts. Immunoblots reported are from one experiment representative of four that gave similar results. β-Tubulin was used as loading control. Density of immunoreactive bands was calculated using the software Quantity one (Bio-Rad) and data are shown as ratio of protein/β-tubulin. Data are expressed as means ± S.D. ($n = 4$; $^*p < 0.001$). (C) Cell number was determined by Trypan Blue exclusion (upper panel) or by MTS assay (bottom panel) 24 and 48 h after treatment with 20 μM H_2O_2. U0126 (260 nM) was added in culture medium 1 h prior H_2O_2 treatment and maintained throughout the experiment. Data are expressed as means ± S.D. ($n = 4$; $^*p < 0.001$).

phospho-active ERK1/2 (p-ERK) by Western blot analysis using a phospho-specific antibody. Fig. 2A shows that no changes in p-ERK1/2 were detected from 6 up to 48 h, times where a significant acceleration of cell growth was observed. ERK1/2 was instead efficiently activated at very early time points starting at 10 min up to 30 min, to finally return to basal level as soon as 1 h from H_2O_2 administration (Fig. 2B). Western blot analysis of basal ERK1/2 showed that its content remained unchanged during all the times screened (Fig. 2B). Among the H_2O_2-sensitive protein kinases possibly stimulating cell proliferation there is also Akt/PKB [28]. Therefore, we attempted to verify whether Akt/PKB could participate in this process. Marker of PKB/Akt activation is its phosphorylation on specific residues [29,30]. Western blot analysis revealed that Akt/PKB was not activated after H_2O_2 administration as it was phosphorylated neither at Ser473 (Fig. 2B) nor at Thr108 (data not shown). To deeply investigate the role played by p-ERK1/2 in H_2O_2-induced cell proliferation, we assessed the effect of U0126, a synthetic ERK1/2 inhibitor, which specifically blocks ERK1/2 phosphorylation by the upstream MEK1/2 kinase. Cell counts by Trypan Blue staining and MTS analysis showed in Fig. 2C indicate that 260 nM U0126 completely abolished the H_2O_2 proliferative effects. These results were also confirmed by BrdU staining (data not shown). Moreover, treatment with U0126 alone led to significant inhibition of cell proliferation at 48 h (Fig. 2C), thus implicating ERK1/2 in the signalling pathway stimulating cell proliferation either upon H_2O_2 treatment or under basal condition. Moreover, U0126 caused a significant reduction in ERK1/2 phosphorylation already in H_2O_2-untreated cells that was maintained during H_2O_2 challenge (Fig. 3A). To further corroborate the involvement of ERK1/2 in H_2O_2-induced proliferation, we measured p-ERK1/2 levels in cells grown in the presence of seleno-methionine. We found that the enrichment of GPx activity, besides inhibiting H_2O_2-induced cell proliferation, inhibited the activation of ERK1/2 as it only slightly accumulated at 15 and 30 min ($p = 0.01$ and $p = 0.02$ respectively) to finally return to basal level at 60 min (Fig. 3B).

3.3. *ERK1/2-c-Jun signalling pathway was responsible for AGS cells proliferation*

We then attempted to delineate the ERK1/2-governed signal transduction activated by H_2O_2, as it can modulate several molecular targets. Many reports demonstrated that c-Jun is among the transcription factors downstream of ERK1/2 governing cell growth and survival. c-Jun involvement was investigated by monitoring both its active phosphorylated form (p-c-Jun) and its translocation into the nuclear compartment. We isolated cell nuclei and we assessed c-Jun content by Western blot. As reported in immunoblot of Fig. 4A, c-Jun started to accumulate at 30 min to subsequently migrate into nuclei after 1 h. After 6 h, c-Jun was almost completely present into nuclear compartment. Since c-Jun transcriptional activity is mainly activated by JNK, we investigated whether this other member of MAPKs family could take part in the process leading to AGS cell proliferation. We hence measured JNK activity by monitoring its phosphorylated form (p-JNK). As illustrated in Fig. 4B, H_2O_2 was not able to induce p-JNK increase, suggesting that only ERK1/2 should be involved in c-Jun activation. To

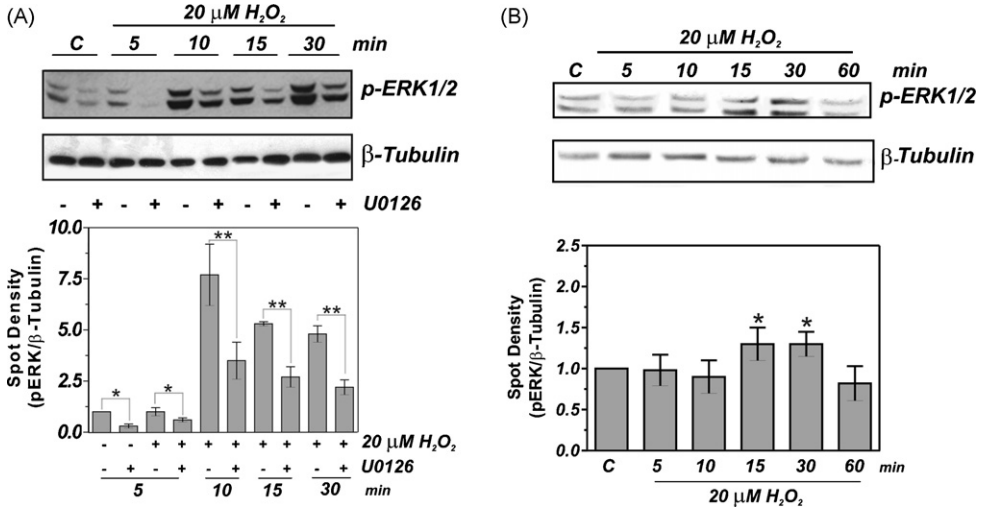

Fig. 3 – MEK1/2 inhibition and GPx overexpression reduce ERK1/2 activation. (A) AGS cells were treated with 20 μM H_2O_2 for the indicated times. p-ERK1/2 protein content was detected by Western blot on total protein extracts. Immunoblots reported are from one experiment representative of four that gave similar results. β-Tubulin was used as loading control. Density of immunoreactive bands was calculated using the software Quantity one (Bio-Rad) and data are shown as ratio of p-ERK/β-tubulin. Data are expressed as means ± S.D. ($n = 4$; $^{*}p < 0.01$, $^{**}p < 0.001$). (B) AGS cells were cultured in the presence of 0.1 μM seleno-methionine for 3 weeks. Medium containing seleno-methionine was removed just before the experiment and replaced with fresh medium. Cells were treated with 20 μM H_2O_2 for the indicated times. p-ERK1/2 protein content was detected by Western blot on total protein extracts. Immunoblots reported are from one experiment representative of five that gave similar results. β-Tubulin was used as loading control. Density of immunoreactive bands was calculated using the software Quantity one (Bio-Rad) and data are shown as ratio of p-ERK/β-tubulin. Data are expressed as means ± S.D. ($n = 5$; $^{*}p < 0.01$).

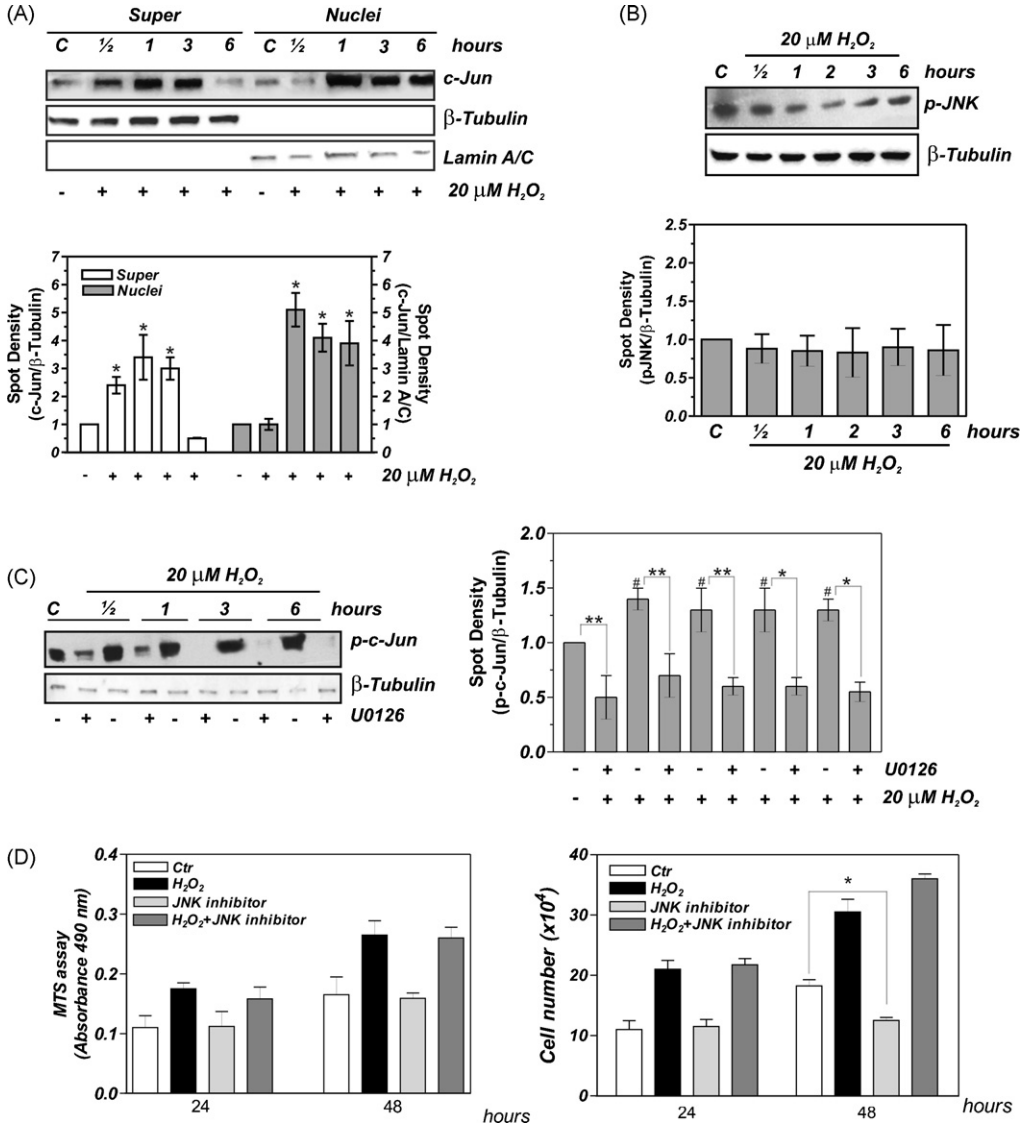

Fig. 4 – ERK1/2 activation promotes c-Jun accumulation, activation and translocation into nuclei. (A) AGS cells were treated with 20 μM H_2O_2 for the indicated times. c-Jun protein content was detected by Western blot on supernatant and nuclear protein extracts. Immunoblots reported are from one experiment representative of four that gave similar results. β-Tubulin and Lamin A/C were used as loading controls. Density of immunoreactive bands was calculated using the software Quantity one (Bio-Rad) and data are shown as ratio of c-Jun/β-tubulin or c-Jun/Lamin A/C. Data are expressed as means ± S.D. ($n = 4$; $^{*}p < 0.001$). (B) p-JNK protein content was detected by Western blot on total cell lysates. β-Tubulin was used as loading control. Immunoblots reported are from one experiment representative of three that gave similar results. Density of immunoreactive bands was calculated using the software Quantity one (Bio-Rad) and data are shown as ratio of p-JNK/β-tubulin. Data are expressed as means ± S.D. ($n = 3$). (C) U0126 (260 nM) was added in culture medium 1 h prior 20 μM H_2O_2 treatment and maintained throughout the experiment. p-c-Jun protein content was detected by Western blot on total cell lysates. β-Tubulin was used as loading control. Immunoblots reported are from one experiment representative of four that gave similar results. Density of immunoreactive bands was calculated using the software Quantity one (Bio-Rad) and data are shown as ratio of p-c-Jun/β-tubulin. Data are expressed as means ± S.D. ($n = 4$; $^{**}p < 0.001$, $^{\#}p < 0.001$ with respect to H_2O_2-untreated cells). (D) Cells number was determined by MTS assay (left panel) or by Trypan Blue exclusion (right panel) 24 h and 48 h after treatment with 20 μM H_2O_2. JNK inhibitor I (10 μM) was added in culture medium 1 h prior H_2O_2 treatment and maintained throughout the experiment. Data are expressed as means ± S.D. ($n = 5$; $^{*}p < 0.05$).

validate this hypothesis, we carried out Western blot analysis of p-c-Jun after ERK1/2 inhibition through U0126. This analysis revealed that p-c-Jun was significantly inhibited by U0126 already in control cells, confirming the influence of ERK1/2 on the phosphorylation state of c-Jun. Importantly, the increase of p-c-Jun triggered by H_2O_2 was dramatically prevented by U0126 both in H_2O_2-treated and untreated cells (Fig. 4C), suggesting that proliferation of AGS cells proceeds via the ERK1/2-c-Jun

route. Cell counts and MTS analysis carried out after treatment with JNK inhibitor finally excluded the involvement of JNK in H_2O_2-simulated cell proliferation (Fig. 4D), although a significant decrease of cell number detected by Trypan Blue staining was found in treatment with JNK I inhibitor alone. The ineffectiveness of JNK inhibitor to block H_2O_2-induced cell proliferation was also confirmed by performing BrdU assay (data not shown).

3.4. *RV blocked the proliferative effects of H_2O_2 in AGS cells by inhibiting ERK1/2 activation*

These data indicated that H_2O_2 evoked cell proliferation via ERK1/2 activation and that this phenomenon was significantly prevented by antioxidants (e.g. catalase, GPx). It has been largely demonstrated that RV exerts an antioxidant action and is an effective and promising anti-proliferative agent that could also act through inhibition of ERK1/2 [23,31,32]. We assessed whether RV could block the proliferative effect of H_2O_2 also in AGS cells. 500 nM RV elicited a prominent inhibition of H_2O_2-evoked cell proliferation at 24 h as assayed by cell counting (data not shown) and by BrdU incorporation analysis (Fig. 5A). Moreover, RV treatment alone was also able to significantly reduce cell proliferation starting at 48 h with a concomitant induction of cell death (Fig. 5B). We then asked whether this polyphenol was able to counteract the proliferative effect of H_2O_2 via an antioxidant action. The intracellular ROS levels were measured by means of cytofluorimetric analysis using the ROS-sensitive probe DCF-DA. We found that ROS significantly increased as early as 5 min, reaching the maximum level at 30 min, to finally return to basal level after 60 min (Fig. 5C). Fig. 5D shows that RV at the concentration of 500 nM was able to lower the intracellular ROS content neither after 30 min from H_2O_2 addition nor under basal condition. The ROS-scavenging capacity of RV was never observed at all the times screened (Fig. 5C), suggesting that it did not exert an antioxidant function under our experimental conditions.

In searching for the mechanism(s) by which RV inhibited cell proliferation, we focused on ERK1/2 signalling pathway. In particular, we determined both p-MEK1/2 and p-ERK1/2 protein levels by Western blot. As showed in Fig. 6A, treatment of AGS cells with 500 nM RV significantly inhibited phosphorylation of ERK1/2 at all the times screened but never interfered with MEK1/2 activation evoked by H_2O_2. In particular, MEK1/2 was activated before ERK1/2 and returned to values close to

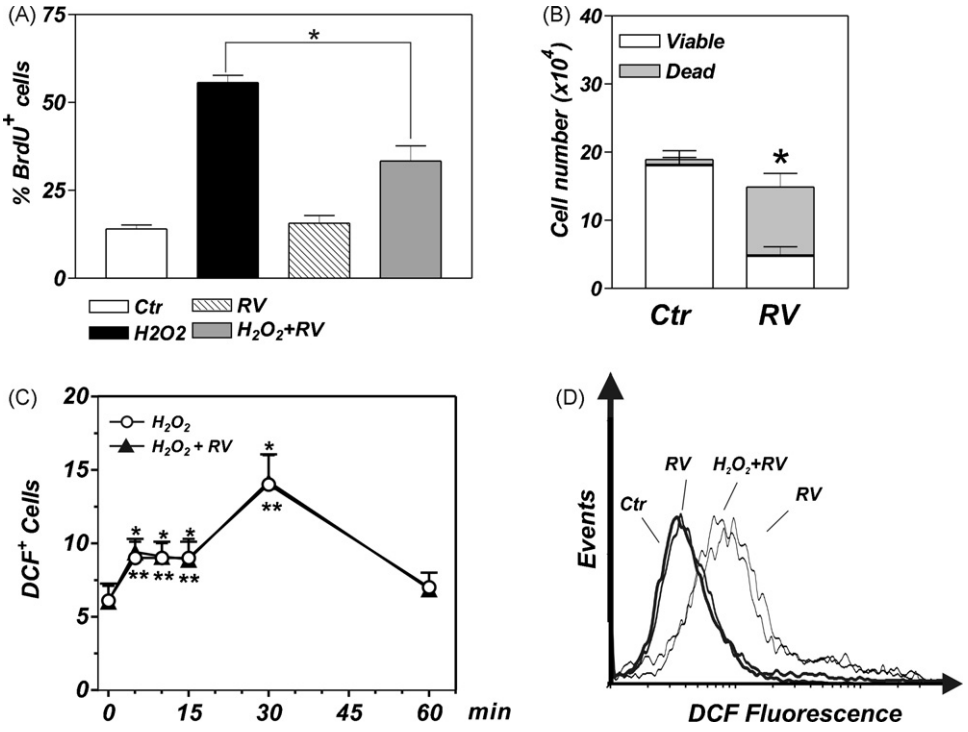

Fig. 5 – RV anti-proliferative effects are not related to its ROS-scavenging capacity. (A) Cell proliferation was determined 6 h after 20 μM H_2O_2 addition through immunofluorescence detection of incorporated BrdU as described under Section 2. RV (500 nM) was added 1 h prior H_2O_2 treatment and maintained throughout the experiment. Data are expressed as means ± S.D. ($n = 3$; $^*p < 0.001$). (B) Cell number was determined by Trypan Blue exclusion 48 h after treatment with 500 nM RV. Data are expressed as means ± S.D. ($n = 4$; $^*p < 0.001$). (C) Cells were incubated with DCF-DA for 1 h and treated with 20 μM H_2O_2 up to 60 min. ROS increase was evaluated measuring DCF fluorescence by cytofluorimetric analysis. Data are reported as percentage of DCF + cells ± S.D. ($n = 6$; $^*p < 0.001$ and $^{**}p < 0.001$ with respect to their own controls (t_0). Differences between H_2O_2 and H_2O2 plus RV are not statistically significant. (D) Cells were incubated with DCF-DA for 1 h. 500 nM RV was added in culture medium 1 h prior 20 μM H_2O_2 treatment and maintained throughout the experiment. ROS increase was evaluated after 30 min measuring DCF fluorescence by cytofluorimetric analysis. Histogram reported is representative of four that gave similar results.

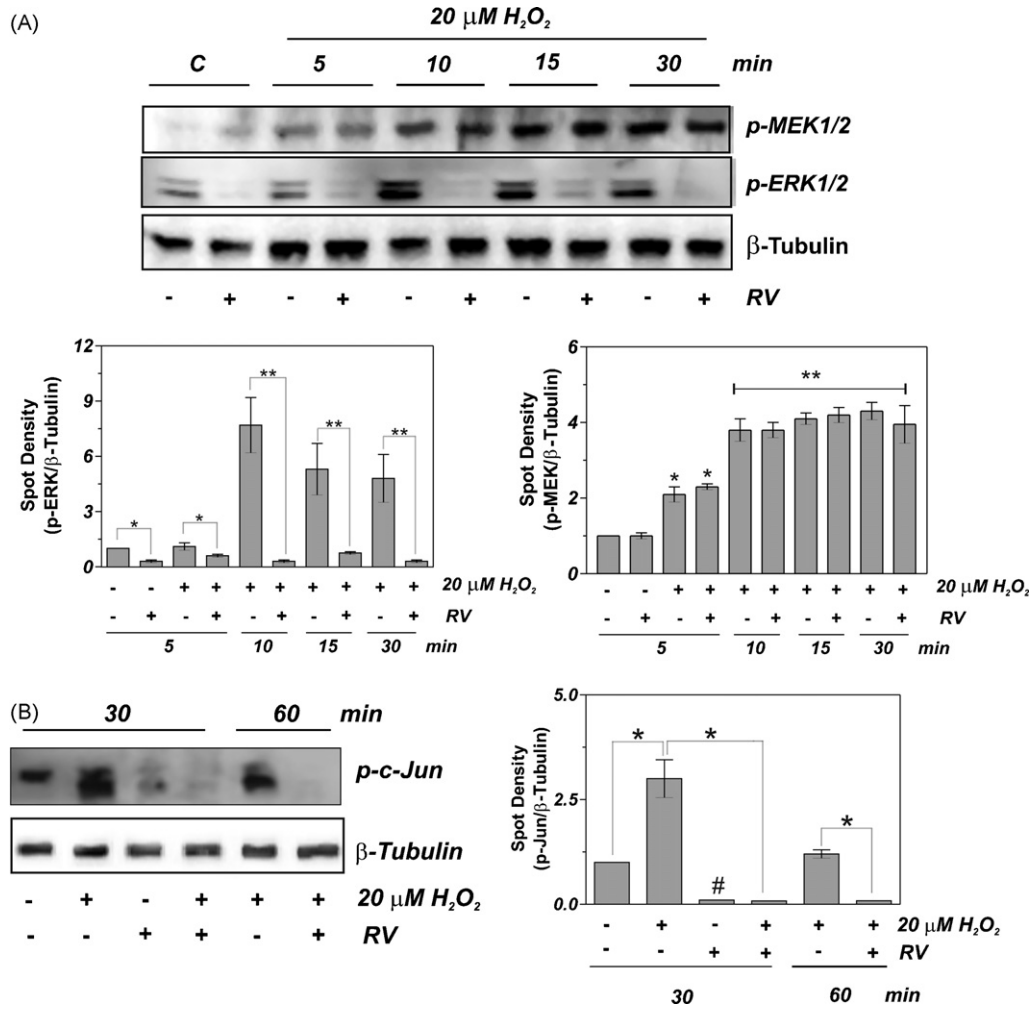

Fig. 6 – RV inhibits H_2O_2-evoked cell proliferation by interfering with MEK1/2-ERK1/2-c-Jun signalling. (A) RV (500 nM) was added in culture medium 1 h prior 20 μM H_2O_2 treatment and maintained throughout the experiment. p-MEK1/2 and p-ERK1/2 protein content was detected by Western blot on total cell lysates. β-Tubulin was used as loading control. Immunoblots reported are from one experiment representative of four that gave similar results. Density of immunoreactive bands was calculated using the software Quantity one (Bio-Rad) and data are shown as ratio of p-MEK/β-tubulin and p-ERK/β-tubulin. Data are expressed as means ± S.D. ($n = 4$; $^{*}p < 0.01$, $^{**}p < 0.001$). (B) RV (500 nM) was added in culture medium 1 h prior 20 μM H_2O_2 treatment and maintained throughout the experiment. p-c-Jun protein content was detected by Western blot on total cell lysates. β-Tubulin was used as loading control. Immunoblots reported are from one experiment representative of four that gave similar results. Density of immunoreactive bands was calculated using the software Quantity one (Bio-Rad) and data are shown as ratio of p-Jun/β-tubulin. Data are expressed as means ± S.D. ($n = 4$, $^{*}p < 0.001$, $^{\#}p < 0.001$ *versus* H_2O_2-untreated cells).

control at 1 h (data not shown). The signalling cascade culminating in c-Jun activation was then examined after RV treatment. Fig. 6B reports immunoblot analysis of p-c-Jun, which demonstrated that c-Jun activation elicited by H_2O_2 was efficiently abrogated by RV both in control and in H_2O_2-treated cells, confirming that the proliferative effects of H_2O_2 are mediated by MEK1/2-ERK1/2-c-Jun signalling axis.

4. Discussion

The dissection of the molecular mechanisms underlying cell proliferation in specific cancer cell types is fundamental for developing more precise and non-invasive anti-cancer therapies. Given that numerous physiologic ligand–receptor interactions leads to H_2O_2 production by mammalian cells, H_2O_2 administration is widely used to mimic oxidation-dependent steps in receptor-mediated signalling pathways, such as that of epidermal growth factor receptor (EGF-R) [6]. In particular, as reported by other authors, H_2O_2 in AGS as well as in other cellular models, mimics some transduction pathways implicated in cell survival and stimulating uncontrolled cell growth [33–35]. In this report we have focused on the signalling pathways activated by H_2O_2 that finally lead to enhanced growth in AGS cells and we have investigated whether low doses of RV could have anti-proliferative effects. We have

evidenced that proliferation of AGS cells proceeds via the recruitment of the ERK1/2-governed signalling pathway. A prompt activation of the ROS-sensitive MEK1/2 and a subsequent canonical MEK1/2-mediated ERK1/2 phosphorylation is elicited as demonstrated by the use of U0126, a specific inhibitor of MEK1/2 kinase activity on ERK1/2. Experiments carried out with U0126 also show that the cross-talk between MEK1/2 and ERK1/2 is a crucial check-point of H_2O_2-promoted AGS cells proliferation as by specifically impeding ERK1/2 phosphorylation the signalling route culminating in c-Jun activation is irreversibly blocked also under basal condition. H_2O_2 stimulus could be spread by the engagement of epidermal growth factor receptor (EGF-R), which has been shown to be activated and aberrantly phosphorylated in the cytosolic interface upon oxidative insult [30]. Whether EGF-R is phosphorylated upon H_2O_2 administration in AGS cells remains to be determined; however, our results indicate that the targets of the H_2O_2 signal lie downstream of the receptor. Experiments carried out in GPx-enriched cells demonstrate that H_2O_2 stimulus is sensed within intracellular milieu since a complete abrogation of H_2O_2-mediated proliferation has been obtained. The H_2O_2 insult in GPx-enriched cells results in a damped, retarded and less persistent ERK1/2 phosphorylation with respect to normal AGS cells. This event is not sufficient for promoting cell replication and is also confirmatory of the strict dependence of AGS cell growth on ERK1/2 signalling [26].

Several substrates have already been discovered for ERK1/2 and many of these are localized in the nucleus as well as in the cytosol. These substrates seem to participate in the regulation of transcription upon stimulation and are responsible for processes such as translation, mitosis and apoptosis [36]. Here, we have proved that the activation of MEK1/2-ERK1/2 by H_2O_2 culminates in c-Jun phosphorylation/activation and its translocation into the nucleus. The analysis of c-Jun localization and phosphorylative status allows us concluding that this signalling pathway is operative and finely orchestrated in space and time as we depicted in Fig. 7. The almost complete absence of c-Jun phosphorylation and inhibition of proliferative stimulus by H_2O_2 upon U0126 treatment, and the lack of PKB/Akt activation demonstrate that in this experimental system the signal is principally transmitted through MEK1/2-ERK1/2-c-Jun axis.

We have also demonstrated that GPx but not RV is able to quench H_2O_2. Albeit RV has been extensively suggested to be capable to scavenge both reactive oxygen and nitrogen species [37], we give proof of the inability of such polyphenol to counteract the oxidative burst triggered by H_2O_2 administration in AGS cells. The lack of an antioxidant action of RV is evidenced by measuring the intracellular ROS content and is confirmed by the result obtained after detecting p-MEK1/2 that remains active regardless of RV. On the contrary, ERK1/2 fails to be activated by H_2O_2 in the presence of RV. The specific inhibitory action of RV on ERK1/2 is still controversial as different hypotheses have been drawn. It has been proposed that RV could interfere with ROS-mediated ERK1/2 phosphorylation as a result of its antioxidant action [31,37] or directly suppress MEK1 activity [23]. Our results point to a site-directed inhibition of MEK1/2 phosphorylation activity on ERK1/2, as a persistent MEK1/2 activation has been found also after RV incubation. This result is in contrast with that obtained by Kim and co-workers, who found that ERK1/2 signalling is blocked by RV upstream of MEK1. The discrepancy could be explained by the higher concentration of RV used by these authors (25–100 μM) that likely could widespread interfere with other phosphorylation steps including Raf1-MEK1 [23]. Indeed, it has been found that RV at lower doses than 25 μM failed to inhibit MEK1 phosphorylation [31]. Lee and co-workers reported that quercetin but not RV can inhibit MEK1 activity probably due to the presence of an additional hydrogen bond, which is the key interaction for stabilizing the inactive conformation of the activation loop of MEK1. These authors did not explore the possible RV action on MEK2 that, although the high homology with MEK1, has a more disordered activation loop with respect to MEK1 [38]. Therefore, in our experimental system, the efficacy of RV to inhibit ERK1/2 phosphorylation could be explained with its specific inhibitory action on MEK2. However, this hypothesis remains to be validated by docking studies and/or *in vitro* kinase assays.

Importantly, we found that RV also inhibits ERK1/2 under basal conditions reinforcing the idea of its direct action on MEK1/2 activity. Notably, the inhibitory effect of RV influences c-Jun activation implying that MEK1/2-ERK1/2 is the principal route involved in AGS cell proliferation. The evidence of a significant cytostatic activity of both U0126 and RV starting at 48 h corroborates this statement. The cytostatic activity is more prominent with RV, in agreement with its highest capacity to inhibit ERK1/2. We can therefore suggest that MEK1/2-ERK1/2-c-Jun signalling is a crucial step for ensuring AGS cell growth not only upon H_2O_2 stimulus but also under steady-state condition.

To our knowledge this is the first case reporting an anti-proliferative effect of RV at so very low doses. Actually, many reports show that only higher concentrations of RV (5–400 μM) are able to efficiently induce cell growth arrest associated with ERK1/2 inhibition in differentiated and other tumour cell types [24,31,39,40]. The bioavailability and stability of polyphenols such as RV, after digestion and blood circulation, is still a debated matter [11,41]. Indeed, RV-conjugates could significantly change biological properties of the original compound. However, it is plausible that the action of RV can be efficiently preserved in stomach milieu, where it can reach higher concentration and accomplish its anti-proliferative action

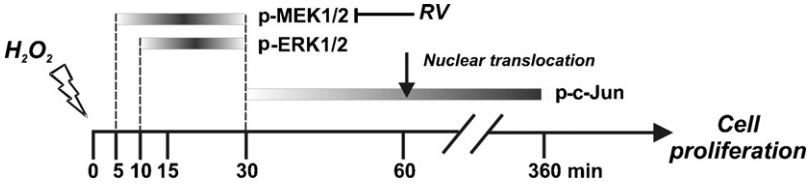

Fig. 7 – Schematic diagram of the events underlying H_2O_2-induced cell proliferation.

directly. Therefore, the high efficiency of RV in impeding cell proliferation at the low doses used in this study might support that it can exert a cancer preventive action also *in vivo*. Finally, our results support the idea that RV can be a weapon for developing new chemopreventive/therapeutic strategies at least for gastric adenocarcinoma management.

Acknowledgments

This work was partially supported by grants from MIUR, FIRB "Idee Progettuali" and Ministero della Salute. We thank Dr. Giuseppe Filomeni for his advice and helpful critical reading of the manuscript.

REFERENCES

[1] Valko M, Leibfritz D, Moncol J, Cronin MT, Mazur M, Telser J. Free radicals and antioxidants in normal physiological functions and human disease. Int J Biochem Cell Biol 2007;39:44–84.
[2] Mattson MP. Effects of microtubule stabilization and destabilization on tau immunoreactivity in cultured hippocampal neurons. Brain Res 1992;582:107–18.
[3] Jackson AL, Loeb LA. The contribution of endogenous sources of DNA damage to the multiple mutations in cancer. Mutat Res 2001;477:7–21.
[4] Hancock JT, Desikan R, Neill SJ. Role of reactive oxygen species in cell signalling pathways. Biochem Soc Trans 2001;29:345–50.
[5] Sauer H, Wartenberg M, Hescheler J. Reactive oxygen species as intracellular messengers during cell growth and differentiation. Cell Physiol Biochem 2001;11:173–86.
[6] Stone JR, Yang S. Hydrogen peroxide: a signaling messenger. Antioxid Redox Signal 2006;8:243–70.
[7] Torres M, Forman HJ. Redox signaling and the MAP kinase pathways. Biofactors 2003;17:287–96.
[8] Turjanski AG, Vaque JP, Gutkind JS. MAP kinases and the control of nuclear events. Oncogene 2007;26:3240–53.
[9] Zhang D, Fan D. Multidrug resistance in gastric cancer: recent research advances and ongoing therapeutic challenges. Expert Rev Anticancer Ther 2007;7:1369–78.
[10] Fry FH, Jacob C. Sensor/effector drug design with potential relevance to cancer. Curr Pharm Des 2006;12:4479–99.
[11] Khan N, Afaq F, Mukhtar H. Cancer chemoprevention through dietary antioxidants: progress and promise. Antioxid Redox Signal 2008;10:475–510.
[12] Surh YJ. Cancer chemoprevention with dietary phytochemicals. Nat Rev Cancer 2003;3:768–80.
[13] Scalbert A, Williamson G. Dietary intake and bioavailability of polyphenols. J Nutr 2000;130:2073S–85S.
[14] de la Lastra CA, Villegas I. Resveratrol as an antioxidant and pro-oxidant agent: mechanisms and clinical implications. Biochem Soc Trans 2007;35:1156–60.
[15] Kundu JK, Surh YJ. Cancer chemopreventive and therapeutic potential of resveratrol: mechanistic perspectives. Cancer Lett 2008;269:243–61.
[16] Wee LM, Long LH, Whiteman M, Halliwell B. Factors affecting the ascorbate- and phenolic-dependent generation of hydrogen peroxide in Dulbecco's Modified Eagles Medium. Free Radic Res 2003;37:1123–30.
[17] Lee KW, Lee HJ. The roles of polyphenols in cancer chemoprevention. Biofactors 2006;26:105–21.
[18] Frei B, Higdon JV. Antioxidant activity of tea polyphenols in vivo: evidence from animal studies. J Nutr 2003;133:3275S–84S.
[19] Heim KE, Tagliaferro AR, Bobilya DJ. Flavonoid antioxidants: chemistry, metabolism and structure-activity relationships. J Nutr Biochem 2002;13:572–84.
[20] Nakagawa T, Yokozawa T. Direct scavenging of nitric oxide and superoxide by green tea. Food Chem Toxicol 2002;40:1745–50.
[21] Lee KW, Kang NJ, Rogozin EA, Kim HG, Cho YY, Bode AM, et al. Myricetin is a novel natural inhibitor of neoplastic cell transformation and MEK1. Carcinogenesis 2007;28:1918–27.
[22] Lee KW, Kang NJ, Heo YS, Rogozin EA, Pugliese A, Hwang MK, et al. Raf and MEK protein kinases are direct molecular targets for the chemopreventive effect of quercetin, a major flavonol in red wine. Cancer Res 2008;68:946–55.
[23] Kim AL, Zhu Y, Zhu H, Han L, Kopelovich L, Bickers DR, et al. Resveratrol inhibits proliferation of human epidermoid carcinoma A431 cells by modulating MEK1 and AP-1 signalling pathways. Exp Dermatol 2006;15:538–46.
[24] El-Mowafy AM, Alkhalaf M, El-Kashef HA. Resveratrol reverses hydrogen peroxide-induced proliferative effects in human coronary smooth muscle cells: a novel signaling mechanism. Arch Med Res 2008;39:155–61.
[25] Baldelli S, Aquilano K, Rotilio G, Ciriolo MR. Glutathione and copper, zinc superoxide dismutase are modulated by overexpression of neuronal nitric oxide synthase. Int J Biochem Cell Biol 2008;40:2660–70.
[26] Filomeni G, Aquilano K, Rotilio G, Ciriolo MR. Glutathione-related systems and modulation of extracellular signal-regulated kinases are involved in the resistance of AGS adenocarcinoma gastric cells to diallyl disulfide-induced apoptosis. Cancer Res 2005;65:11735–42.
[27] Lowry OH, Rosebrough NJ, Farr AL, Randall RJ. Protein measurement with the Folin phenol reagent. J Biol Chem 1951;193:265–75.
[28] Mehdi MZ, Azar ZM, Srivastava AK. Role of receptor and nonreceptor protein tyrosine kinases in H_2O_2-induced PKB and ERK1/2 signaling. Cell Biochem Biophys 2007;47:1–10.
[29] Radisavljevic ZM, Gonzalez-Flecha B. TOR kinase and Ran are downstream from PI3K/Akt in H_2O_2-induced mitosis. J Cell Biochem 2004;91:1293–300.
[30] Khan EM, Lanir R, Danielson AR, Goldkorn T. Epidermal growth factor receptor exposed to cigarette smoke is aberrantly activated and undergoes perinuclear trafficking. FASEB J 2008;22:910–7.
[31] King RE, Kent KD, Bomser JA. Resveratrol reduces oxidation and proliferation of human retinal pigment epithelial cells via extracellular signal-regulated kinase inhibition. Chem Biol Interact 2005;151:143–9.
[32] Delmas D, Lancon A, Colin D, Jannin B, Latruffe N. Resveratrol as a chemopreventive agent: a promising molecule for fighting cancer. Curr Drug Targets 2006;7:423–42.
[33] Hocker M, Rosenberg I, Xavier R, Henihan RJ, Wiedenmann B, Rosewicz S, et al. Oxidative stress activates the human histidine decarboxylase promoter in AGS gastric cancer cells. J Biol Chem 1998;273:23046–54.
[34] Goldkorn T, Balaban N, Matsukuma K, Chea V, Gould R, Last J, et al. EGF-Receptor phosphorylation and signaling are targeted by H_2O_2 redox stress. Am J Respir Cell Mol Biol 1998;19:786–98.
[35] Goldkorn T, Ravid T, Khan EM. Life and death decisions: ceramide generation and EGF receptor trafficking are modulated by oxidative stress. Antioxid Redox Signal 2005;7:119–28.
[36] Yoon S, Seger R. The extracellular signal-regulated kinase: multiple substrates regulate diverse cellular functions. Growth Factors 2006;24:21–44.

[37] Aquilano K, Baldelli S, Rotilio G, Ciriolo MR. Role of nitric oxide synthases in Parkinson's disease: a review on the antioxidant and anti-inflammatory activity of polyphenols. Neurochem Res 2008;33:2416–26.
[38] Ohren JF, Chen H, Pavlovsky A, Whitehead C, Zhang E, Kuffa P, et al. Structures of human MAP kinase kinase 1 (MEK1) and MEK2 describe novel noncompetitive kinase inhibition. Nat Struct Mol Biol 2004;11:1192–7.
[39] Lee B, Moon SK. Resveratrol inhibits TNF-alpha-induced proliferation and matrix metalloproteinase expression in human vascular smooth muscle cells. J Nutr 2005;135: 2767–73.
[40] Tang FY, Chiang EP, Sun YC. Resveratrol inhibits heregulin-beta1-mediated matrix metalloproteinase-9 expression and cell invasion in human breast cancer cells. J Nutr Biochem 2008;19:287–94.
[41] Jannin B, Menzel M, Berlot JP, Delmas D, Lancon A, Latruffe N. Transport of resveratrol, a cancer chemopreventive agent, to cellular targets: plasmatic protein binding and cell uptake. Biochem Pharmacol 2004;68:1113–8.